

Discrete sampling of extreme events modifies their statistics

Lior Zarfaty,¹ Eli Barkai,¹ and David A. Kessler²

¹Department of Physics, Institute of Nanotechnology and Advanced Materials, Bar-Ilan University, Ramat-Gan 52900, Israel

²Department of Physics, Bar-Ilan University, Ramat-Gan 52900, Israel

Extreme value (EV) statistics of correlated systems are widely investigated in diverse fields like weather forecasting and earthquakes prediction. Does the unavoidable discrete sampling (DS) of a continuous correlated stochastic process change its EV distribution? We explore this question for correlated random variables modeled via Langevin dynamics for a particle in a symmetric potential $U(x)$. We find that for long measurement times, when $\lim_{x \rightarrow \infty} x/U(x) = 0$ the EV distribution of the DS process diverges from the continuous prediction and instead converges to that originating from independent and identically distributed random variables drawn from the process' equilibrium measure. The above condition includes Weibull and certain Gumbel processes, but not Fréchet ones. Our findings show that the EV statistics can be extremely sensitive to the sampling rate of the data.

Introduction. Extreme value (EV) statistics is a venerable branch of probability theory, which has drawn much interest over the years [1–5]. It finds diverse application not only in physics [6–40], but in many other fields of science as well [41–58]. Predicting when will the next EV event occur and of what magnitude it will be is practically important, as the extremes are typically the scenarios we are looking forward to, or alternatively, must watch out for [26, 27, 43, 44, 54]. Hence, a thorough understanding of EV statistics is crucial. The EV distribution arising from independent and identically distributed (IID) random variables (RV) has various limiting laws when the sample size approaches infinity [59–63], in a similar way to central limit theorems for sums of IID RVs [64]. More precisely, the nature of the tail of the underlying distribution of the IID RVs determines the limiting form of the scaled EV's distribution to be either a Gumbel, a Fréchet, or a Weibull. However, it is clear that for many natural processes correlations are vital and omnipresent [34], hence the assumption that one is dealing with IID RVs is, in most cases, simply wrong [7, 12, 19, 20, 26, 29, 37, 39].

Typically, one measures an extreme of a time series that represents some quantity, be it for example a temperature [55], the value of a currency [57], or the position of an active biological entity [58]. In principle, the series is continuous, and EV models of such continuously sampled (CS) stochastic paths have attracted considerable attention. However, in reality, for any experimental study the amount of data collected and the sampling rate of the measurement devices are both always finite. Thus, the approach that is relevant to real-world applications is to first discretely sample (DS) the path, and then find the maximum of the sampled sequence of data. Is there a major difference between these two sampling methods?

In this Letter, we answer this question in the context of correlated trajectories of a Brownian particle in a force field, modeled by Langevin dynamics. We start with one of the most well-investigated stochastic processes, the Ornstein-Uhlenbeck (OU) model [see also 30, 65]. It describes the motion of an overdamped particle in an harmonic field or, equivalently, the velocity of an under-

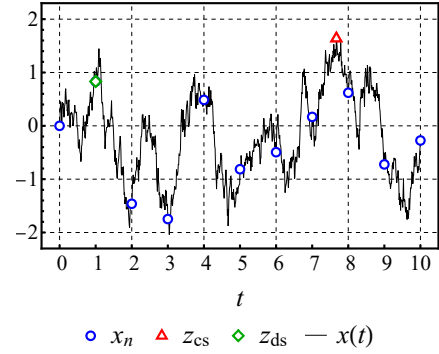


FIG. 1. (Color online) The trajectory of a Brownian particle in a confining harmonic force, modeled via the OU process. The maximum of this path is z_{cs} (red triangle), while a DS every $\Delta = 1$ units of time yields the sequence x_n (blue circles), with a maximum of z_{ds} (green diamond).

damped Brownian particle. Naively, if the time between sampling events is shorter than the relaxation time, then the former should not be expected to play a major role, and we expect to get the CS EV statistics. But, as we show here, for any finite sampling interval this is wrong.

Our remarkable finding is a qualitative non-smooth transition from DS to CS in the statistics of extremes, which we present first using the OU model. It exists for any positive sampling interval when the overall measurement time is increased, and is not related to a physical change of the system. It strongly affects the mean and variance of the EV distribution, and thus also the typical fluctuations and large deviations of the EVs [38]. Nevertheless, for the OU process both DS and CS belong to the Gumbel domain, see below.

We then extend our results to a wide class of Langevin processes that lie in the Gumbel domain, unveiling a second transition governed by the large-displacement behavior of the force field controlling the dynamics. Finally, within this Langevin approach, we briefly present extensions to processes that belong to the other two EV limits, Fréchet and Weibull.

The Ornstein-Uhlenbeck model. We start by considering the Langevin equation for the OU model,

$$\frac{d}{dt}x(t) = -\frac{1}{\tau}x(t) + \sqrt{2D}\eta(t), \quad (1)$$

where τ , D , and $\eta(t)$ are the relaxation time, the diffusion coefficient, and the standard Gaussian white noise, respectively. The noise obeys $\langle \eta(t)\eta(t') \rangle = \delta(t-t')$ and has zero mean, where $\delta(\cdot)$ is Dirac's delta function. The path $x(t)$ is subjected to a force which is derived from a quadratic potential. We rescale all quantities in the equation such that t and $x(t)$ are measured in units of τ and $\sqrt{D\tau}$, respectively. We specialize to this OU path $x(t)$ in the time interval $[0, T]$, and sample it stroboscopically every Δ units of time, see Fig. 1. The outcome of this DS measurement is the random sequence $x_n \equiv x(n\Delta)$, where $0 \leq n \leq N$ and $N\Delta = T$ is the total measurement time. We focus on the maximum of this set, denoted z_{ds} , and compare its properties to those of the previously studied case of the maximum of $x(t)$ in the interval $[0, T]$, $z_{\text{cs}} \equiv \max_{0 \leq t \leq T} [x(t)]$ [34]. To compute this latter quantity, one has to measure the whole continuous trajectory and hence we call it the CS model. Clearly, $z_{\text{ds}} \leq z_{\text{cs}}$.

The binding force ensures that an ensemble of particles will reach a steady state, the Boltzmann-Gibbs measure, given by $\phi(x) \equiv \exp(-x^2/2)/\sqrt{2\pi}$. In the limit of large Δ and T but fixed N , the sampling is of uncorrelated RVs all drawn from the equilibrium distribution (ED). Thus, if $z_{\text{ds}} < z$ then all the N sampled variables are also smaller than z , and since they are IID RVs drawn from the ED we find that $\lim_{\Delta \rightarrow \infty} \text{Prob}(z_{\text{ds}} < z) = [\Phi(z)]^N$, with $\Phi(z) \equiv \int_{-\infty}^z dx \phi(x) = 1 - \text{erfc}(z/\sqrt{2})/2$ and $\text{erfc}(\cdot)$ is the complementary error function. In this limit, the nature of the EV statistics is only due to the equilibrium properties of the system, and any dynamical information such as the correlation effects is wiped out. Note that when N is large the typical EVs are also large [38], hence we assume $z \gg 1$, where $\Phi(z) \simeq 1 - z^{-1}\phi(z)$, and get

$$\lim_{\Delta \rightarrow \infty} \text{Prob}(z_{\text{ds}} < z) \sim \exp[-Nz^{-1}\phi(z)]. \quad (2)$$

To treat the DS EV case, we consider the path's values at the moments of sampling x_n using a discrete stochastic map. By integrating the Langevin equation, Eq. (1), one finds the OU update formula, $x_{n+1} = \mu x_n + \sqrt{1-\mu^2}\eta_n$, with η_n a standard Gaussian deviate and $\mu = \exp(-\Delta)$ [66]. In the large- N limit, we find

$$\text{Prob}(z_{\text{ds}} < z) \sim A(z) \exp\left\{-N \ln\left[\frac{1}{\Lambda_*(z)}\right]\right\}. \quad (3)$$

The amplitude $A(z)$ approaches unity for large z and the main focus here is the largest eigenvalue closest to one in magnitude, $\Lambda_*(z)$. The latter obeys the following integral equation, obtained from the stochastic map [67],

$$\Lambda_*(z)P_*(x; z) = \int_{-\infty}^z \frac{dx' P_*(x'; z)}{\sqrt{2\pi(1-\mu^2)}} \exp\left[-\frac{(x-\mu x')^2}{2(1-\mu^2)}\right], \quad (4)$$

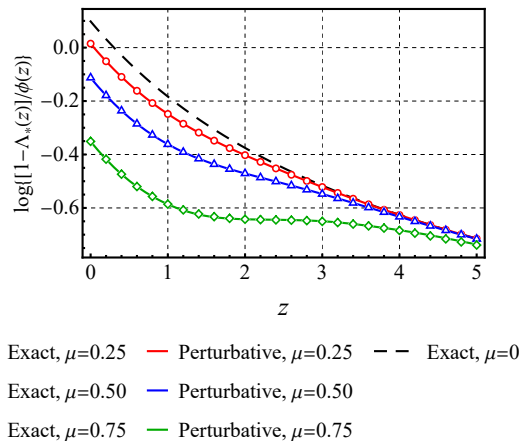


FIG. 2. (Color online) The scaled eigenvalue $[1 - \Lambda_*(z)]/\phi(z)$ for $\mu = 0.25$ (red circles), $\mu = 0.5$ (blue triangles), and $\mu = 0.75$ (green diamonds), obtained from numerical evaluations of the eigenvalue equation, Eq. (4), as well as from a 10th-order expansion in μ (solid curves). Also shown is the exact result for the IID case, $\mu = 0$, for which $\Lambda_*(z) = \Phi(z)$ (dashed black line). Note that all three finite- μ curves merge for large z with the IID curve.

where $P_*(x; z)$ is the corresponding eigenfunction. Evaluating the joint limit of $\Delta \rightarrow 0$ and $N \rightarrow \infty$ with T fixed and large [67], we obtain the Fokker-Planck description of the problem, $\lim_{\Delta \rightarrow 0} \text{Prob}(z_{\text{ds}} < z) \sim \exp[-T\lambda_*(z)]$, i.e., the CS limit, with $\lambda_*(z) \equiv \lim_{\Delta \rightarrow 0} [1 - \Lambda_*(z)]/\Delta$. In Ref. [34], it was shown that $\lambda_*(z)$ is the smallest magnitude solution of $D_{\lambda_*(z)}(-z) = 0$, $D(\cdot)$ being the parabolic cylinder function, a result which we recover. For large z , one has $\lambda_*(z) \sim z\phi(z)$ [68], and the CS limit becomes

$$\lim_{\Delta \rightarrow 0} \text{Prob}(z_{\text{ds}} < z) \sim \exp[-Tz\phi(z)]. \quad (5)$$

The Gaussian decay of the exponents in Eqs. (2) and (5) means that both the IID and CS limits belong to the Gumbel universality class. However, the large- z asymptotic behavior of these two exponents differ by a diverging factor of z^2 , making the corresponding EV distributions vastly different. Surprisingly, for any finite Δ , the large- N limit of the DS process' EV distribution, Eq. (3), which is dominated by the large- z asymptotics of the eigenvalue $\Lambda_*(z)$, converges to the EV measure given by the ED IID limit, both for the OU process along with a wide class of similar processes, as we show below. Hence, the limit of $\Delta \rightarrow 0$ is singular in the context of EV theory.

To begin analyzing the DS EV problem, we use a small- μ (or alternatively, large Δ) perturbation theory, expanding $\Lambda_*(z) = \sum_{n=0}^{\infty} \lambda_n(z)\mu^n$, and similarly for $P_*(x; z)$. Using Eq. (4), we get that $\Lambda_*(z) \simeq \Phi(z) + \mu[\phi(z)]^2/\Phi(z)$ to first order in μ . For large- z this implies that

$$\Lambda_*(z) \simeq 1 - z^{-1}\phi(z) + \mu[\phi(z)]^2. \quad (6)$$

The second term is expected as it is the result obtained for IID RVs that originate from the ED. A key observa-

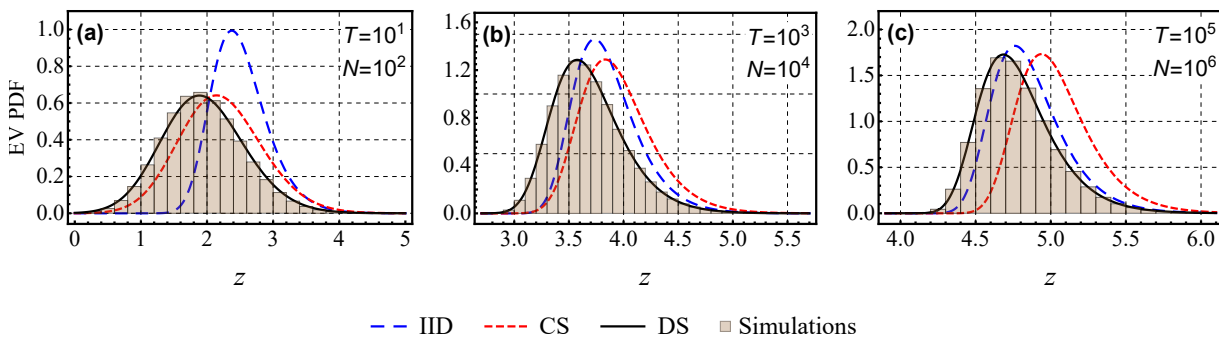


FIG. 3. (Color online) The distribution of EVs for the DS OU process, with $\Delta = 0.1$. For not too large T , we see a behavior close to that of the CS approach, see panel (a). However, as we increase T , approximating the DS statistics by those of CS becomes less accurate, see panel (b), and eventually approaches the statistics predicted for $N = T/\Delta$ IID RVs drawn from the ED, see panel (c). The IID and DS curves (dashed blue and solid black) correspond to $\exp\{-N \ln[1/\Lambda(z)]\}$ with $\Lambda(z) = \Phi(z)$ and $\Lambda(z) = \Lambda_*(z)$, respectively. The CS curve (short-dashed red) corresponds to $\exp[-T\lambda_*(z)]$, where $D_{\lambda_*(z)}(-z) = 0$. Each histogram is made of 10^6 maxima whose initial conditions are $x = 0$, evolving via the stochastic map $x_{n+1} = \mu x_n + \sqrt{1 - \mu^2} \eta_n$.

tion is that for large z , the third term is by far smaller than the second one, even if μ is not too small, since $\phi(z) \ll 1$. The first-order correction with μ is thus exponentially small in z with respect to the leading term. We continue the small- μ expansion to order 10 [69] and find, similarly, that all the terms up to μ^{10} are negligible in the large- z limit. This behavior is also found in numerical calculations of the eigenvalue $\Lambda_*(z)$ [67], as exhibited in Fig. 2, showing that for large values of z all the numerical data converge to a unique curve which is Δ independent, namely the IID curve. This suggests that when z is large the EV statistics will converge to that of IID RVs drawn from the ED for any positive Δ .

To prove this claim, we need a different strategy that exploits the large- z expansion of the integral eigenvalue equation, i.e., Eq. (4). Expressing the largest eigenvalue as $\Lambda_*(z) \simeq 1 - \phi(z)\Lambda_1(z) + [\phi(z)]^2\Lambda_2(z)$, and similarly for $P_*(x; z)$, we obtain [67]

$$\Lambda_*(z) \simeq 1 - \phi(z) \underbrace{\frac{\text{erfc}(z/\sqrt{2})}{2\phi(z)}}_{\Lambda_1(z)} + [\phi(z)]^2 \underbrace{\sum_{n=1}^{\infty} \frac{\mu^n/n!}{1-\mu^n} \text{He}_{n-1}^2(z)}_{\Lambda_2(z)}, \quad (7)$$

where $\text{He}_n(\cdot)$ is the n th probabilists' Hermite polynomial. Further expanding Eq. (7) for large z , we find

$$\begin{aligned} \Lambda_*(z) &\simeq 1 - \frac{\phi(z)}{z} + \left[\frac{\phi(z)}{z} \right]^2 \frac{(1+\mu)^2}{\sqrt{1-\mu^2}} \exp\left(\frac{z^2\mu}{1+\mu}\right) \\ &\simeq 1 - \frac{\phi(z)}{z} \left(1 - \frac{2e^{-\Delta z^2/4}}{\sqrt{\pi\Delta z^2}} \right), \end{aligned} \quad (8)$$

where the last expression is valid for small Δ [70]. Remarkably, the leading two terms are μ independent and

correspond to the result for IID variables originating from the ED. However, for fixed z , when Δ becomes small, or equivalently μ approaches unity, the last term diverges, indicating the breakdown of the large- z perturbation theory and the existence of a crossover regime to a CS behavior for $\Delta z^2 \sim \mathcal{O}(1)$. This is evidenced in Fig. 3, where one sees that for small $T = \Delta N$, the distribution of z_{ds} is close to the CS prediction, whereas for large T it appears to converge to the IID limit. This transition has however nothing to do with a physical switch of the behavior of the system, and is rather a purely statistical effect due to the finite sampling rate. Thus, for any fixed $\Delta > 0$, as T becomes large the IID statistics and ED control the EV theory.

A qualitative argument. How are we to understand the crossover scale of $\Delta z^2 \sim \mathcal{O}(1)$? A simple explanation to this result is as follows. Let us expand the recursion relation of x_n for small Δ , $x_{n+1} - x_n \simeq -\Delta x_n + \sqrt{2\Delta}\eta_n$. We see that there is a competition between two terms. For small Δ the stochastic noise is dominant, and so a record-breaking large x_n is very liable to be followed by a yet larger value. However, for sufficiently large x_n , the deterministic term which is proportional to x_n dominates, so those maxima are separated by large gaps in time. These two terms are comparable precisely in the crossover regime we have identified. Physically, the effect we find here is related to the fact that extreme events of Langevin paths in a confining field become larger as time progresses. However, the bigger is the true maximum (in the CS sense), the faster the relaxation from this extreme gets, simply because the restoring force field gets enormously large if the path wanders to an EV. This idea suggests that our main result found for the OU process is of more general validity. We explore this by considering the path of a Brownian particle subjected to more general binding force fields. As explained below, these results go beyond the Gumbel basin of attraction.

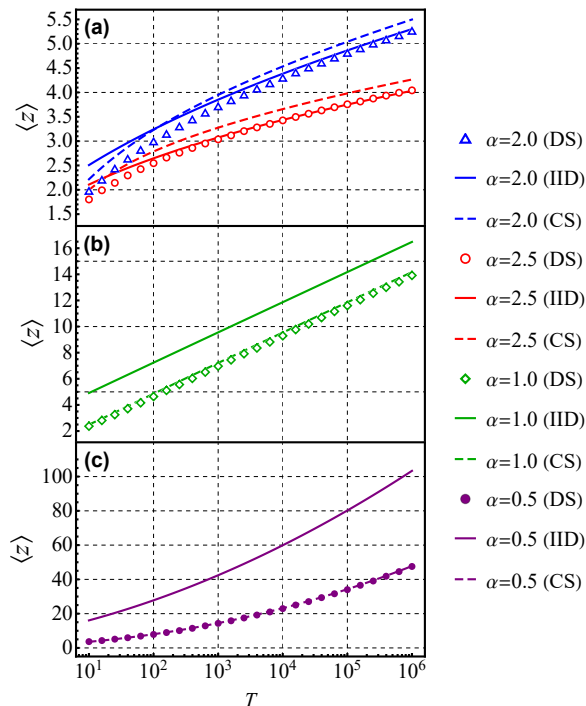


FIG. 4. (Color online) The mean EV $\langle z \rangle$ of a DS process $x(t)$, evolving according to Eq. (1) but with a deterministic force of $-U'(x)$, where $U(x) = (1/\alpha)(1+x^2)^{\alpha/2}$. We used (a) $\alpha = 2$ and $\alpha = 2.5$ (blue triangles and red circles, respectively), (b) $\alpha = 1$ (green diamonds), and (c) $\alpha = 0.5$ (purple disks), corresponding to the OU model, to an additional example of an increasing-force process, and to two counterexamples, a constant and a decreasing force, respectively. Seen are numerical evaluations for the four cases, where the sampling interval is $\Delta = 0.1$. Also depicted are the ED IID (solid lines) and CS (dashed curves) predictions for each value of α . For $\alpha > 1$, the DS values converge to the IID description, see panel (a). The opposite happens for $\alpha < 1$, as this case has a force that vanishes for large distances, see panel (c). The borderline case is $\alpha = 1$, where the DS, IID, and CS values do not seem to intersect, see panel (b). Each mean is made of 10^4 maxima whose initial conditions are $x = 0$, obtained using the Euler-Maruyama method with an underlying time increment of 0.01. A reflective boundary condition at $x = 0$ was used when $\alpha < 1$. Further details regarding this figure appear in [67].

Other force fields in the Gumbel domain. Let us consider a potential of the form $U(x) = (1/\alpha)(1+x^2)^{\alpha/2}$, with $\alpha > 0$ (see further details in [67]). In Fig. 4, we plot the mean EV $\langle z \rangle$ versus T given various values of α . For the OU process with $\alpha = 2$, we see that the numerical values converge to the IID limit at large times, see panel (a). This works also for $\alpha = 2.5$, since here too the force grows with x , leading to a domination by the deterministic force term at long times. This argument is no longer valid for $\alpha \leq 1$, where the force does not increase with x , see panels (b) and (c). For example, when setting $\alpha = 0.5$, the stochastic term dominates at large x and the exact values (which are nicely described by CS) di-

verge from the IID behavior, see panel (c). When $\alpha = 1$, the force is asymptotically constant, which is a special borderline case with all curves being parallel, see panel (b). This case was also shown to be critical for problems which do not involve DS, see Ref. [14] in the context of crowding of near-extreme events, and Ref. [71] where a freezing transition was discovered for the long-time decay rates of first-passage probabilities.

The Fréchet and Weibull EV limits. Until now, we discussed processes with an asymptotic power-law potential. This means EDs of exponential type, and as such, their EV limits belong to the Gumbel class. However, our observations hold for the other two EV basins of attraction as well. Firstly, consider a potential which grows logarithmically for large displacements [72–74], $U(x) = (\beta/2) \ln(1+x^2)$ with $\beta > 1$. Here, the ED decays as a power-law, hence the IID limit belongs to the Fréchet class. We observe a behavior similar to the above case of $\alpha < 1$. Namely, due to the force diminishing at infinity, the DS EV distribution, studied numerically via its mode z_0 , agrees with the CS prediction. Secondly, consider a potential corresponding to a particle diffusing in a box, $U(x) = 0$ for $0 \leq x \leq L$ and $U(x) = \infty$ otherwise. Since here the ED has a finite upper support point, the IID limit belongs to the Weibull class. For this case we find that $L - \langle z \rangle$ converges towards the IID prediction of $\propto 1/T$ for large T , which is vastly different than the CS prediction, i.e., an exponential decay with T . Derivations of these results, supporting figures, and additional extensions appear in [67]. We thus conjecture that any process with a potential obeying $\lim_{x \rightarrow \infty} x/U(x) = 0$ will have its long-time limit controlled by the ED IID behavior.

Summary and conclusions. We demonstrated how the difference between DS and CS affects the EV distribution of correlated RVs generated from Langevin paths. For the OU process, we found that large measurement times yield statistics of IIDs drawn from the ED for any nonzero sampling interval. After providing an intuitive explanation as to why this happens, we showed it holds for a class of potential fields that are strongly binding. We demonstrated that this is not true for the complementary cases, where the EV distribution diverges from that of IID RVs. Lastly, we showed that our findings apply also to the other two classical limits of EVs, Fréchet and Weibull, which were studied via two example cases.

The profound sensitivity of the EV theory of correlated continuous processes to the method of sampling suggests that similar effects will be present also in more general models. Further, changes in the statistics of EVs can be related to the sampling problem found here, and not to a real change in the physical properties of the system, as we explained. Exploring these issues for models such as fractional Brownian motion, continuous time random walks, processes with demographic or multiplicative noise, and statistics of first-passage times of DS processes remains an open challenge.

Acknowledgments. The support of the Israel Science Foundation via grant number 1614/21 is acknowledged.

-
- [1] E. J. Gumbel, *Statistics of Extremes* (Dover, New York 1958).
- [2] M. R. Leadbetter, G. Lindgren, and H. Rootzen, *Extremes and Related Properties of Random Sequences and Processes* (Springer-Verlag, New York, 1982).
- [3] S. Kotz and S. Nadarajah, *Extreme Value Distributions: Theory and Applications* (Imperial College Press, London, 2000).
- [4] S. Coles, *An Introduction to Statistical Modeling of Extreme Values* (Springer, London, 2001).
- [5] L. de Haan and A. Ferreira, *Extreme Value Theory: An Introduction* (Springer, New York, 2006).
- [6] J. P. Bouchaud and M. Mézard, *J. Phys. A: Math. Gen.* **30** 7997 (1997).
- [7] D. S. Dean and S. N. Majumdar, *Phys. Rev. E* **64**, 046121 (2001).
- [8] T. Antal, M. Droz, G. Györgyi, and Z. Rácz, *Phys. Rev. Lett.* **87**, 240601 (2001).
- [9] S. N. Majumdar and P. L. Krapivsky, *Phys. Rev. E* **65** 036127 (2002).
- [10] A. Comtet and S. N. Majumdar, *J. Stat. Mech.*, P06013 (2005).
- [11] E. Bertin, *Phys. Rev. Lett.* **95** 170601 (2005).
- [12] E. Bertin and M. Clusel, *J. Phys. A: Math. Gen.* **39** 7607 (2006).
- [13] D. S. Dean and S. N. Majumdar, *Phys. Rev. Lett.* **97**, 160201 (2006).
- [14] S. Sabhapandit and S. N. Majumdar, *Phys. Rev. Lett.* **98**, 140201 (2007).
- [15] G. Biroli, J. P. Bouchaud, and M. Potters, *J. Stat. Mech.*, P07019 (2007).
- [16] D. S. Dean and S. N. Majumdar, *Phys. Rev. E* **77**, 041108 (2008).
- [17] M. R. Evans and S. N. Majumdar, *J. Stat. Mech.*, P05004 (2008).
- [18] Y. V Fyodorov and J. P. Bouchaud *J. Phys. A: Math. Theor.* **41** 372001 (2008).
- [19] G. Györgyi, N. R. Moloney, K. Ozogány, and Z. Rácz, *Phys. Rev. Lett.* **100**, 210601 (2008).
- [20] S. N. Majumdar and R. M. Ziff, *Phys. Rev. Lett.* **101**, 050601 (2008).
- [21] S. N. Majumdar, A. Comtet, and J. R. Furling, *J. Stat. Phys.* **138**, 955 (2010).
- [22] G. Györgyi, N. R. Moloney, K. Ozogány, Z. Rácz, and M. Droz, *Phys. Rev. E* **81**, 041135 (2010).
- [23] E. Bertin, *J. Phys. A: Math. Theor.* **43** 345002 (2010).
- [24] E. Bertin and G. Györgyi, *J. Stat. Mech.*, P08022 (2010).
- [25] I. I. Eliazar and I. M. Sokolov, *Phys. A: Stat. Mech. Appl.* **389**, 4462 (2010).
- [26] G. Wergen, *J. Phys. A: Math. Theor.* **46**, 223001 (2013).
- [27] J. Y. Fortin and M. Clusel, *J. Phys. A: Math. Theor.* **48**, 183001 (2015).
- [28] A. Bar, S. N. Majumdar, G. Schehr, and D. Mukamel, *Phys. Rev. E* **93**, 052130 (2016).
- [29] O. Bénichou, P. L. Krapivsky, C. Mejía-Monasterio, and G. Oshanin, *Phys. Rev. Lett.* **117**, 080601 (2016).
- [30] D. Hartich and A. Godec, *J. Phys. A: Math. Theor.* **52**, 244001 (2019).
- [31] A. Vezzani, E. Barkai, and R. Burioni *Phys. Rev. E.* **100**, 012108 (2019).
- [32] W. Buijsman, V. Gritsev, and V. Cheianov, *Phys. Rev. B* **100**, 205110 (2019).
- [33] W. Wang, A. Vezzani, R. Burioni, and E. Barkai, *Phys. Rev. Res.* **1**, 033172 (2019).
- [34] S. N. Majumdar, A. Pal, and G. Schehr, *Phys. Rep.* **840**, 1 (2020).
- [35] M. Höll, W. Wang, and E. Barkai, *Phys. Rev. E* **102**, 042141 (2020).
- [36] C. Godrèche, *J. Stat. Phys.* **182**, 13 (2021).
- [37] D. S. Grebenkov, V. Sposini, R. Metzler, G. Oshanin, and F. Seno, *New J. Phys.* **23** 023014 (2021).
- [38] L. Zarfaty, E. Barkai, and D. A. Kessler, *J. Phys. A: Math. Theor.* **54**, 315205 (2021).
- [39] B. De Bruyne, S. N. Majumdar, and G. Schehr, *J. Stat. Mech.*, 083215 (2021).
- [40] F. Mori, S. N. Majumdar, and G. Schehr, *Europhys. Lett.* **135**, 30003 (2021).
- [41] P. C. Y. Chen and Y.C. Fung, *Microvasc. Res.* **6** 32 (1973).
- [42] P. W. Burton, *Geophys. J. Int.* **59** 249 (1979).
- [43] F. Rossi, M. Fiorentino, and P. Versace, *Water Resour. Res.* **20**, 847 (1984).
- [44] D. Sornette, L. Knopoff, Y. Y. Kagan, and C. Vanneste, *J. Geophys. Res.* **101**, 13883 (1996).
- [45] P. Embrechts, C. Klüppelberg, and T. Mikosch, *Modelling Extremal Events for Insurance and Finance* (Springer, Berlin, 1997).
- [46] P. Embrechts, S. I. Resnick, and G. Samorodnitsky, *N. Am. Actuar. J.* **3**, 2 (1999).
- [47] R. W. Katz, M. B. Parlange, and P. Naveau, *Adv. Water Resour.* **25** 1287 (2002).
- [48] H. A. Orr, *Genetics* **163**, 1519 (2003).
- [49] P. Naveau, M. Nogaj, C. Ammann, P. Yiou, D. Cooley, and V. Jomelli, *C. R. Geosci* **337**, 1013 (2005).
- [50] G. Gradoni and L. R. Arnaut, *IEEE Trans. Electromagn. Compat.* **52** 506 (2010).
- [51] E. Castillo, *Extreme Value Theory in Engineering* (Elsevier, 2012).
- [52] S. M. Papalexiou and D. Koutsoyiannis, *Water Resour. Res.* **49** 187 (2013).
- [53] E. Ben-Naim, E. G. Daub, and P. A. Johnson, *Geophys. Res. Lett.* **40** 3021 (2013).
- [54] I. A. Chaves and R. E. Melchers, *Struct. Saf.* **50** 9 (2014).
- [55] L. Cheng, A. AghaKouchak, E. Gilleland, and R. W. Katz, *Clim. Change* **127** 353 (2014).
- [56] D. K. Dey and J. Yan, *Extreme Value Modeling and Risk Analysis: Methods and Applications* (CRC Press, 2016).
- [57] J. Osterrieder and J. Lorenz, *Ann. Financ. Econ.* **12** 1750003 (2017).
- [58] Z. Schuss, K. Basnayake, and D. Holcman, *Phys. Life Rev.* **28**, 52 (2019).
- [59] L. H. C. Tippett and R. A. Fisher, *Proc. Cambridge Phil. Soc.* **24**, 180 (1928).
- [60] E. J. Gumbel *Ann. Inst. Henri Poincaré* **5** 115 (1935).
- [61] B. V. Gnedenko, *Ann. Math.* **44**, 423 (1943).
- [62] P. Hall, *J. App. Prob.* **16**, 433 (1979).
- [63] R. Giuliano and C. Macci, *Comm. Stat.* **43**, 1077

- (2014).
- [64] B. V. Gnedenko and A. N. Kolmogorov, *Limit Distributions for Sums of Independent Random Variables* (Addison-Wesley, Cambridge, 1968).
- [65] M. J. Kearney and R. J. Martin, *J. Phys. A: Math. Theor.* **54** 055002 (2021).
- [66] D. T. Gillespie, *Phys. Rev. E* **54**, 2084 (1996).
- [67] See the supplemental material for (I) Further details regarding Eq. (4); (II) Derivation of Eqs. (7) and (8); and (III) Langevin processes with non-linear forces.
- [68] Note that in Ref. [34], a typographical error resulted in an extra factor of two (S. N. Majumdar, private communication).
- [69] Wolfram Research Inc., Mathematica, Version 12.1.1, Champaign, IL (2020).
- [70] Note that the $\Delta \rightarrow 0$ limit of Eq. (5) yields the CS picture for any z . However, the $z \rightarrow \infty$ limit of Eq. (8) holds only for not-too-small Δ . Since these limits do not commute, the obtained expressions are different.
- [71] S. Sabhapandit and S. N. Majumdar, *Phys. Rev. Lett.* **125**, 200601 (2020).
- [72] H. C. Fogedby and R. Metzler, *Phys. Rev. Lett.* **98**, 070601 (2007).
- [73] A. Dechant, E. Lutz, E. Barkai, and D. A. Kessler, *J. Stat. Phys.* **145**, 1524 (2011).
- [74] O. Hirschberg, D. Mukamel, and G. M. Schütz, *Phys. Rev. E* **84** (2011).

Supplemental material for: Discrete sampling of extreme events modifies their statistics

Lior Zarfaty,¹ Eli Barkai,¹ and David A. Kessler²

¹*Department of Physics, Institute of Nanotechnology and Advanced Materials, Bar-Ilan University, Ramat-Gan 52900, Israel*

²*Department of Physics, Bar-Ilan University, Ramat-Gan 52900, Israel*

In what follows, equations and figures that are numbered without the prefix “SM” refer to their main text counterparts.

FURTHER DETAILS REGARDING EQ. (4)

Obtaining the stochastic map

We start from the rescaled Langevin equation

$$\frac{d}{dt}x(t) = -x(t) + \sqrt{2}\eta(t), \quad (\text{SM1})$$

where $\eta(\cdot)$ corresponds to the standard Gaussian white noise, obeying $\langle \eta(t)\eta(t') \rangle = \delta(t-t')$ and having a zero mean, with $\delta(\cdot)$ denoting the delta function of Dirac. The time t lies in the interval $[0, T]$, where T is the overall measurement duration. With $x(0)$ denoting the initial condition, this equation has the following solution,

$$x(t) = e^{-t}x(0) + \sqrt{2} \int_0^t dt' e^{t'-t}\eta(t'), \quad (\text{SM2})$$

which can be easily verified by differentiation. For some $\Delta > 0$, Eq. (SM2) can be brought to the following form,

$$x(t + \Delta) = e^{-\Delta}x(t) + \sqrt{2} \int_0^\Delta dt' e^{t'-\Delta}\eta(t + t'). \quad (\text{SM3})$$

A discrete sampling (DS) of step Δ means that one deals with the sequence $\{x_0, x_1, \dots, x_N\}$, where $n \equiv t/\Delta$, $x_n \equiv x(\Delta n)$, and $N \equiv T/\Delta$. Then, we can rewrite Eq. (SM3) as

$$x_{n+1} = e^{-\Delta}x_n + \eta_n, \quad \eta_n \equiv \sqrt{2} \int_0^\Delta dt' e^{t'-\Delta}\eta(t + t'), \quad (\text{SM4})$$

where η_n is a Gaussian random variable (RV) with mean 0 and a variance of $1 - \exp(-2\Delta)$ (see below), independent of x_m for $m \leq n$ and of η_m for $m \neq n$.

Derivation of Eq. (4)

Starting with some distribution for the initial condition $x_0 = x(0)$, denoted by $P_0(x)$, the distribution of an x_n obtained after n iterations of Eq. (SM4), denoted by $P_n(x)$, satisfies

$$P_n(x) \equiv \text{Prob}(x_n = x) = \int_{-\infty}^{\infty} dx' \text{Prob}(x_{n-1} = x' \wedge \eta_{n-1} = x - e^{-\Delta}x') = \int_{-\infty}^{\infty} dx' P_{n-1}(x')K(x - e^{-\Delta}x'), \quad (\text{SM5})$$

where $K(\cdot)$ is the probability density function (PDF) of the independent and identically distributed (IID) RVs $\{\eta_n\}$. Clearly, the DS extreme value (EV) $z_{\text{ds}} \equiv \max_{0 \leq n \leq N}(x_n)$ is smaller than z if and only if all the x_n s are less than z . The recurrence equation governing this event is obtained by replacing $P_n(x) \rightarrow \theta(z-x)P_n(x; z)$ in Eq. (SM5), where $\theta(\cdot)$ is the Heaviside step function, yielding

$$P_n(x; z) = \theta(z-x) \int_{-\infty}^z dx' P_{n-1}(x'; z)K(x - e^{-\Delta}x'). \quad (\text{SM6})$$

Equation (SM6) is a linear map from $P_{n-1}(x; z)$ to $P_n(x; z)$, and so it is solvable by an eigenvalue expansion, $P_n(x; z) = \sum_{\Lambda} A_{\Lambda}(z) \Lambda^n(z) P_{\Lambda}(x; z)$. Due to the cutoff at z , probability is lost in each iteration, and the eigenvalues are all smaller than unity. Thus, for large n , the expansion is dominated by the ground state eigenvalue $\Lambda_*(z)$ and eigenfunction $P_*(x; z)$, which obey Eq. (4),

$$\Lambda_*(z) P_*(x; z) = \int_{-\infty}^z dx' P_*(x'; z) K(x - e^{-\Delta} x'). \quad (\text{SM7})$$

Note that redefining the domain of x to be $(-\infty, z]$ allows us to discard the Heaviside step function.

Finding the kernel

To obtain the kernel of Eq. (4), namely the PDF of the RV η_n , we calculate the characteristic function of η_n using path integral formalism,

$$\langle e^{ik\eta_n} \rangle = \int \mathcal{D}\eta \exp \left[i\sqrt{2}k \int_0^{\Delta} dt' e^{t'-\Delta} \eta(t+t') \right] = \prod_{t'} \int_{-\infty}^{\infty} d\eta \phi(\eta) \exp \left(i\sqrt{2}e^{t'-\Delta} k\eta \right), \quad (\text{SM8})$$

where the continuous noise's PDF is given by the standard Gaussian distribution,

$$\phi(\eta) \equiv \frac{e^{-\eta^2/2}}{\sqrt{2\pi}}. \quad (\text{SM9})$$

Thus, we find

$$\langle e^{ik\eta_n} \rangle = \prod_{t'} \exp \left[-e^{2(t'-\Delta)} k^2 \right] = \exp \left[-k^2 \int_0^{\Delta} dt' e^{2(t'-\Delta)} \right] = \exp \left(-\frac{1 - e^{-2\Delta}}{2} k^2 \right). \quad (\text{SM10})$$

Finally, when inverted back to position space, these yield

$$K(\xi) = \frac{1}{\sqrt{1 - \mu^2}} \phi \left(\frac{\xi}{\sqrt{1 - \mu^2}} \right), \quad (\text{SM11})$$

where $\mu \equiv \exp(-\Delta)$.

The $\Delta \rightarrow 0$ limit

The long-time behavior of the continuous sampling (CS) limit can be retrieved from Eq. (4) by taking $\Delta \rightarrow 0$, leading to $\mu \simeq 1 - \Delta$ and $\Lambda_*(z) \simeq 1 - \Delta \lambda_*(z)$. Changing variables to $\chi = (x - \mu x')/\sqrt{1 - \mu^2}$ in the integration and expanding for $\Delta \rightarrow 0$ gives

$$P_*(x; z) \simeq P_*(x; z) + \Delta \begin{cases} [1 + \lambda_*(z)] P_*(x; z) + x \frac{d}{dx} P_*(x; z) + \frac{d^2}{dx^2} P_*(x; z) & x < z \\ -\frac{1}{2\Delta} P_*(z; z) & x = z \end{cases}. \quad (\text{SM12})$$

Hence, $p_*(x; z) \equiv \lim_{\Delta \rightarrow 0} P_*(x; z)$ satisfies the differential equation

$$\frac{d^2}{dx^2} p_*(x; z) + \frac{d}{dx} \left[p_*(x; z) x \right] + \lambda_*(z) p_*(x; z) = 0, \quad (\text{SM13})$$

with a boundary condition at $x = z$ of $p_*(z; z) = 0$, yielding the solution

$$p_*(x; z) \propto \exp \left(-\frac{x^2}{4} \right) D_{\lambda_*(z)}(-x), \quad D_{\lambda_*(z)}(-z) = 0, \quad (\text{SM14})$$

exactly as in Ref. [SM1]. A derivation of long-time asymptotics of the CS limit for a general Langevin potential field appears below (third section).

Numerical solutions

Numerically, it proves useful to work with representations of the eigenfunction and eigenvalue that are based on their large- z asymptotics. Therefore, we start with making the following substitution,

$$\tilde{P}_*(x; z) \equiv 1 - \frac{P_*(x; z)}{P_*(x; \infty)}, \quad \tilde{\Lambda}_*(z) \equiv 1 - \Lambda_*(z), \quad (\text{SM15})$$

where $P_*(x; \infty) \equiv \lim_{z \rightarrow \infty} P_*(x; z)$, and of course $\lim_{z \rightarrow \infty} \Lambda(z) = 1$. The solution at $z \rightarrow \infty$ can be found by a Fourier transform of the eigenvalue equation, giving $P_*(x; \infty) = \phi(x)$. The integral eigenvalue equation then becomes

$$\left[1 - \tilde{\Lambda}_*(z)\right] \phi(x) \left[1 - \tilde{P}_*(x; z)\right] = \int_{-\infty}^z dx' \phi(x') K(x - \mu x') - \int_{-\infty}^z dx' \phi(x') \tilde{P}_*(x'; z) K(x - \mu x'), \quad (\text{SM16})$$

where the left integral can be performed analytically. Next, we note that taking $z \rightarrow \infty$ has a similar mathematical consequence as having $x \rightarrow -\infty$. Hence, let us assume that for some negative x_m with $|x_m| \gg 1$, we can write an iterative approximation for the solution of Eq. (SM16),

$$\tilde{P}_*(x; z) \approx \begin{cases} \tilde{P}_n^*(x; z) & x_m \leq x \leq z \\ 0 & -\infty < x < x_m \end{cases}, \quad (\text{SM17})$$

where $\tilde{P}_n^*(x; z)$ is the $[x_m, z]$ -part of the eigenfunction corresponding to the n th iteration. Similarly, we denote $\tilde{\Lambda}_n^*(z)$ as the n th iteration's eigenvalue. Thus, for $x \in [x_m, z]$, Eq. (SM16) changes to

$$\left[1 - \tilde{\Lambda}_n^*(z)\right] \phi(x) \left[1 - \tilde{P}_n^*(x; z)\right] = \int_{-\infty}^z dx' \phi(x') K(x - \mu x') - \int_{x_m}^z dx' \phi(x') \tilde{P}_{n-1}^*(x'; z) K(x - \mu x'). \quad (\text{SM18})$$

Assuming $\tilde{P}_{n-1}^*(x; z)$ is known, we discretize x' on the interval $[x_m, z]$ and calculate the right integral of Eq. (SM18). We find $\tilde{\Lambda}_n^*(z)$ by evaluating Eq. (SM18) at $x = x_m$, where due to continuity $\tilde{P}_n^*(x_m; z) = 0$, yielding

$$\left[1 - \tilde{\Lambda}_n^*(z)\right] \phi(x) = \int_{-\infty}^z dx' \phi(x') K(x_m - \mu x') - \int_{x_m}^z dx' \phi(x') \tilde{P}_{n-1}^*(x'; z) K(x_m - \mu x'). \quad (\text{SM19})$$

Using this value, we obtain $\tilde{P}_n^*(x; z)$ for $x \in [x_m, z]$. Starting with $\tilde{P}_0^*(x; z) = 0$ and continuing to iterate gives a series of approximations to $\tilde{P}_*(x; z)$ which converges efficiently. The left integral of Eqs. (SM18) and (SM19) can be expressed in a simple closed form, and we get

$$\begin{aligned} \tilde{\Lambda}_n^*(z) &= \frac{1}{2} \operatorname{erfc} \left[\frac{z - \mu x_m}{\sqrt{2(1 - \mu^2)}} \right] + \int_{x_m}^z dx' \frac{\tilde{P}_{n-1}^*(x'; z)}{\sqrt{2\pi(1 - \mu^2)}} \exp \left[-\frac{(x' - \mu x_m)^2}{2(1 - \mu^2)} \right], \\ \tilde{P}_n^*(x; z) &= \left[1 - \tilde{\Lambda}_n^*(z)\right]^{-1} \left\{ \frac{1}{2} \operatorname{erfc} \left[\frac{z - \mu x}{\sqrt{2(1 - \mu^2)}} \right] + \int_{x_m}^z dx' \frac{\tilde{P}_{n-1}^*(x'; z)}{\sqrt{2\pi(1 - \mu^2)}} \exp \left[-\frac{(x' - \mu x)^2}{2(1 - \mu^2)} \right] - \tilde{\Lambda}_n^*(z) \right\}. \end{aligned} \quad (\text{SM20})$$

Lastly, we define a measure of convergence to determine the stopping point of this iterative process,

$$\mathcal{E} \equiv \left| \frac{\tilde{\Lambda}_{100m}^*(z)}{\tilde{\Lambda}_{100(m-1)}^*(z)} - 1 \right|, \quad 1 < m \in \mathbb{N}. \quad (\text{SM21})$$

This prescription was used to obtain the numerical data for $\Lambda_*(z)$ presented in Figs. 2 and 3. The discretization step in x was 0.01, and we used $x_m = -5$ and $\mathcal{E} = 10^{-7}$.

DERIVATION OF EQS. (7) AND (8)

We start by writing that for large- z

$$P_*(x; z) \simeq \phi(x) \left\{ 1 + \phi(z) \mathcal{P}_1(x; z) + [\phi(z)]^2 \mathcal{P}_2(x; z) \right\}, \quad \Lambda_*(z) \simeq 1 - \phi(z) \Lambda_1(z) + [\phi(z)]^2 \Lambda_2(z). \quad (\text{SM22})$$

These expansions are to be understood in the context of a fixed $0 \leq \mu < 1$.

Finding the first-order correction

Plugging the above expansion into Eq. (4), we get to first order

$$\phi(x) [1 + \phi(z)\mathcal{P}_1(x; z) - \phi(z)\Lambda_1(z)] = \int_{-\infty}^z dx' \phi(x') \frac{1 + \phi(z)\mathcal{P}_1(x'; z)}{\sqrt{2\pi(1-\mu^2)}} \exp\left[-\frac{(x-\mu x')^2}{2(1-\mu^2)}\right]. \quad (\text{SM23})$$

The zeroth-order equation is satisfied since

$$\int_{-\infty}^z dx' \phi(x') \frac{1}{\sqrt{2\pi(1-\mu^2)}} \exp\left[-\frac{(x-\mu x')^2}{2(1-\mu^2)}\right] = \phi(x) \left\{ 1 - \frac{1}{2} \operatorname{erfc}\left[\frac{z-x\mu}{\sqrt{2(1-\mu^2)}}\right] \right\}, \quad (\text{SM24})$$

where $\operatorname{erfc}(\cdot)$ is the complementary error function. Using the following expansion [SM2] of the Gaussian kernel function of Eq. (4), which holds for $0 \leq \mu < 1$,

$$\frac{1}{\sqrt{2\pi(1-\mu^2)}} \exp\left[-\frac{(x-x'\mu)^2}{2(1-\mu^2)}\right] = \phi(x) \sum_{n=0}^{\infty} \frac{\mu^n}{n!} \operatorname{He}_n(x) \operatorname{He}_n(x'), \quad (\text{SM25})$$

where $\operatorname{He}_n(\cdot)$ is the n th probabilists' Hermite polynomial, we obtain to first order

$$\mathcal{P}_1(x; z) - \Lambda_1(z) + \frac{1}{2\phi(z)} \operatorname{erfc}\left[\frac{z-x\mu}{\sqrt{2(1-\mu^2)}}\right] - \int_{-\infty}^{\infty} dx' \phi(x') \mathcal{P}_1(x'; z) \sum_{n=0}^{\infty} \frac{\mu^n}{n!} \operatorname{He}_n(x) \operatorname{He}_n(x') = 0. \quad (\text{SM26})$$

Note that we have extended the integral's boundary to infinity, dropping a higher-order correction to be accounted for during the second-order calculation. Exploiting another expansion [SM3] similar to the one above,

$$\operatorname{erfc}\left[\frac{z-x\mu}{\sqrt{2(1-\mu^2)}}\right] = \operatorname{erfc}\left(\frac{z}{\sqrt{2}}\right) + 2\phi(z) \sum_{n=1}^{\infty} \frac{\mu^n}{n!} \operatorname{He}_n(x) \operatorname{He}_{n-1}(z), \quad (\text{SM27})$$

together with expressing the first functional correction as a sum over Hermite polynomials in x ,

$$\mathcal{P}_1(x; z) = \sum_{n=0}^{\infty} c_n(z) \operatorname{He}_n(x), \quad (\text{SM28})$$

and using their orthogonality condition (where $\delta_{n,m}$ is the Kronecker delta),

$$\int_{-\infty}^{\infty} dx' \phi(x') \operatorname{He}_n(x') \operatorname{He}_m(x') = \delta_{n,m} n!, \quad (\text{SM29})$$

we get for the first-order expansion

$$\left[c_0(z) (1 - \mu^0) - \Lambda_1(z) + \frac{1}{2\phi(z)} \operatorname{erfc}\left(\frac{z}{\sqrt{2}}\right) \right] \operatorname{He}_0(x) + \sum_{n=1}^{\infty} \left[c_n(z) (1 - \mu^n) + \frac{\mu^n}{n!} \operatorname{He}_{n-1}(z) \right] \operatorname{He}_n(x) = 0. \quad (\text{SM30})$$

Thus, we obtain

$$\Lambda_1(z) = \frac{\operatorname{erfc}(z/\sqrt{2})}{2\phi(z)}, \quad c_n(z) = -\frac{\mu^n}{n!} \frac{\operatorname{He}_{n-1}(z)}{1 - \mu^n}, \quad n > 0, \quad (\text{SM31})$$

where $\Lambda_1(z) \sim z^{-1}$ for $z \rightarrow \infty$. The value of $c_0(z)$ can be found from the condition $\mathcal{P}_1(0; z) = 0$, since an x -independent addition to $\mathcal{P}_1(x; z)$ is just a change of normalization. This yields

$$c_0(z) = -\sum_{n=1}^{\infty} c_n(z) \operatorname{He}_n(0) = -\sum_{n=1}^{\infty} \frac{\sqrt{\pi} 2^{n/2} c_n(z)}{\Gamma[(1-n)/2]}, \quad (\text{SM32})$$

where $\Gamma(\cdot)$ is the gamma function.

Obtaining the second-order correction

Since we have an exact solution of the first-order equation, we can move on to the second order. We further expand Eq. (4) to second-order, obtaining

$$\begin{aligned} \mathcal{P}_2(x; z) - \mathcal{P}_1(x; z)\Lambda_1(z) + \Lambda_2(z) + \frac{1}{\phi(z)} \int_z^\infty dx' \phi(x') \mathcal{P}_1(x'; z) \sum_{n=0}^{\infty} \frac{\mu^n}{n!} \text{He}_n(x) \text{He}_n(x') \\ - \int_{-\infty}^\infty dx' \phi(x') \mathcal{P}_2(x'; z) \sum_{n=0}^{\infty} \frac{\mu^n}{n!} \text{He}_n(x) \text{He}_n(x') = 0. \end{aligned} \quad (\text{SM33})$$

The first integral term is the higher-order correction that was dropped in Eq. (SM26). As done above, the boundary of the second integral term was extended to infinity (since the contribution from $x' > z$ only enters the calculation of the third-order correction). Let us express $\mathcal{P}_2(x; z)$ similarly to its first-order counterpart,

$$\mathcal{P}_2(x; z) = \sum_{n=0}^{\infty} d_n(z) \text{He}_n(x). \quad (\text{SM34})$$

Plugging this and Eq. (SM31) into Eq. (SM33) and rearranging, we get from the terms which multiply $\text{He}_0(x)$ that

$$\Lambda_2(z) = \sum_{n=1}^{\infty} \frac{\mu^n/n!}{1-\mu^n} \phi_{n,0}(z) \text{He}_{n-1}(z), \quad (\text{SM35})$$

with [SM4]

$$\phi_{n,m}(z) \equiv \frac{1}{\phi(z)} \int_z^\infty dx \phi(x) \text{He}_n(x) \text{He}_m(x) = \sum_{l=0}^L l! \binom{n}{l} \binom{m}{l} \text{He}_{n+m-2l-1}(z) + \delta_{n,m} n! \frac{\text{erfc}(z/\sqrt{2})}{2\phi(z)}, \quad (\text{SM36})$$

where $L \equiv \min(n, m) - \delta_{n,m}$ and we used the standard convention that a summation from 0 to -1 vanishes. Taking $m = 0$ and $n \geq 1$, we get $\phi_{n,0}(z) = \text{He}_{n-1}(z)$, hence

$$\Lambda_2(z) = \sum_{n=1}^{\infty} \frac{\mu^n/n!}{1-\mu^n} \text{He}_{n-1}^2(z), \quad (\text{SM37})$$

which, together with $\Lambda_1(z)$ from Eq. (SM31), yields Eq. (7) when plugged into Eq. (SM22). Finally, using the identity

$$\sum_{n=0}^{\infty} \frac{\nu^n}{n!} \text{He}_n^2(z) = \frac{1}{\sqrt{1-\nu^2}} \exp\left(\frac{z^2\nu}{1+\nu}\right), \quad (\text{SM38})$$

which arises in the calculation of the density of states of the finite temperature quantum harmonic oscillator [SM5], we find

$$\Lambda_2(z) = \sum_{n=1}^{\infty} \int_0^{\mu^n} \frac{d\nu}{\sqrt{1-\nu^2}} \exp\left(\frac{z^2\nu}{1+\nu}\right) \underset{z \rightarrow \infty}{\sim} \frac{(1+\mu)^2}{\sqrt{1-\mu^2}} z^{-2} \exp\left(\frac{z^2\mu}{1+\mu}\right). \quad (\text{SM39})$$

Together with the asymptotic behavior of $\Lambda_1(z)$ at infinity, the top row of Eq. (8) is obtained.

LANGEVIN PROCESSES WITH NON-LINEAR FORCES

Here we provide further details regarding the generalization of our findings to different Langevin equations. We start with generalizing Eq. (1),

$$\frac{d}{dt} x(t) = -\frac{D}{K_B \mathcal{T}} U'[x(t)] + \sqrt{2D} \eta(t), \quad (\text{SM40})$$

where $U(x)$ is the potential, D is the diffusion coefficient, K_B is Boltzmann's constant, \mathcal{T} is the temperature, $\eta(t)$ is the same standard Gaussian white noise as defined above, and primes denote derivatives. Note that we take the

potential to be an even function of x . The equilibrium distribution of this process is given by the Boltzmann-Gibbs measure,

$$P_{\text{eq}}(x) = \frac{1}{Z} \exp \left[-\frac{U(x)}{K_B \mathcal{T}} \right], \quad Z \equiv \int_{-\infty}^{\infty} dx \exp \left[-\frac{U(x)}{K_B \mathcal{T}} \right], \quad (\text{SM41})$$

where Z is the partition function. Therefore, the IID limit for the EV cumulative distribution function (CDF) is

$$F_N^{\text{IID}}(z) \equiv \lim_{\Delta \rightarrow \infty} \text{Prob}(z_{\text{ds}} < z) = \left[\int_{-\infty}^z dx P_{\text{eq}}(x) \right]^N. \quad (\text{SM42})$$

On the other hand, the CS limit is obtainable by the method described in Ref. [SM1] for the Ornstein-Uhlenbeck (OU) process, which is in fact extremely general and goes beyond this specific model. The main idea is to solve the Fokker-Planck representation of Eq. (SM40),

$$\frac{\partial}{\partial t} p(x, t|z) = D \frac{\partial^2}{\partial x^2} p(x, t|z) + \frac{D}{K_B \mathcal{T}} \frac{\partial}{\partial x} \left[p(x, t|z) U'(x) \right], \quad (\text{SM43})$$

with an initial condition of $p(x, 0|z) = \delta(x)$ and boundary conditions of $p(-\infty, t|z) = p(z, t|z) = 0$. Here, the notation $p(x, t|z)$ denotes the probability for a particle described by $x(t)$ to arrive at x on time t , while always staying below the value z . The EV CDF at the total measurement time T is then

$$F_T^{\text{CS}}(z) \equiv \lim_{\Delta \rightarrow 0} \text{Prob}(z_{\text{ds}} < z) = \text{Prob}(z_{\text{cs}} < z) = \int_{-\infty}^z dx p(x, T|z). \quad (\text{SM44})$$

Formally, one can write a solution via an eigenvalue expansion,

$$p(x, t|z) = \sum_{\lambda} A_{\lambda}(z) e^{-D\lambda(z)t} p_{\lambda}(x; z), \quad (\text{SM45})$$

where $\{\lambda(z)\}$ are the eigenvalues and $\{p_{\lambda}(x; z)\}$ are the eigenfunctions, which obey

$$\frac{d^2}{dx^2} p_{\lambda}(x; z) + \frac{d}{dx} \left[p_{\lambda}(x; z) \frac{U'(x)}{K_B \mathcal{T}} \right] + \lambda(z) p_{\lambda}(x; z) = 0, \quad (\text{SM46})$$

with boundary conditions of $p_{\lambda}(-\infty; z) = p_{\lambda}(z; z) = 0$. Let us denote as $\lambda_*(z)$ and $p_*(x; z)$ the smallest eigenvalue and its associated eigenfunction. Note that for $z \rightarrow \infty$ we have $\lambda_*(z) \rightarrow 0$, which is to be expected since in this limit the boundary conditions of $p_*(x; z)$ yield the equilibrium density $P_{\text{eq}}(x)$, associated with a zero eigenvalue. Thus, in the long measurement time limit $t = T \rightarrow \infty$, we can replace $p_*(x; z)$ with $P_{\text{eq}}(x)$ and set $A_* = 1$ (due to the initial condition being normalized), which yields

$$F_T^{\text{CS}}(z) \sim \exp[-D\lambda_*(z)T], \quad (\text{SM47})$$

up to exponentially small corrections.

Below we consider three example cases, classified according to the large N limit of Eq. (SM42). Our aim is to find the IID and CS representations of the EV distribution of the DS process for the three EV basins of attraction. Using these limiting functions, we verify the general nature of our study.

The Gumbel class

The Gumbel class occurs when $-\ln[P_{\text{eq}}(x)] \propto x^{\alpha}$ for $x \rightarrow \infty$ and $\alpha > 0$. Accordingly, here we assume a potential with an asymptotic behavior of

$$U(x) \propto |x|^{\alpha}, \quad \alpha > 0, \quad (\text{SM48})$$

for $x \rightarrow \pm\infty$. As mentioned in the main text, the DS EV distribution displays two different behaviors depending on the value of α , and therefore, we split our derivation of the CS limit into two. Starting with $\alpha > 1$, we solve Eq. (SM46) for $x \in (-\infty, z]$ with boundary conditions of $p_*(-\infty; z) = 0$ and $p_*(z; z) = 0$, from which $\lambda_*(z)$ emerges. We do so by

using perturbation theory around $\lambda_*(z) = 0$, for which $z \rightarrow \infty$ as mentioned above. Writing $p_*(x) = p_0^*(x) + p_1^*(x; z)$, Eq. (SM46) reads for the zeroth order

$$\frac{d^2}{dx^2} p_0^*(x) + \frac{d}{dx} \left[p_0^*(x) \frac{U'(x)}{K_B \mathcal{T}} \right] = 0, \quad (\text{SM49})$$

whose general solution is

$$p_0^*(x) = C_1 y_1(x) + C_2 y_2(x) \quad (\text{SM50})$$

where

$$y_1(x) \equiv \exp \left[-\frac{U(x)}{K_B \mathcal{T}} \right], \quad y_2(x) \equiv y_1(x) \int_0^x d\xi \exp \left[\frac{U(\xi)}{K_B \mathcal{T}} \right], \quad (\text{SM51})$$

with boundary conditions of $p_0^*(-\infty) = p_0^*(\infty) = 0$. Since $y_2(x)$ decays algebraically when $x \rightarrow \pm\infty$, more precisely $y_2(x) \propto |x|^{1-\alpha}$, it needs to be discarded, as the solution should approach zero for $x \rightarrow -\infty$ in an exponential manner. Therefore, we have

$$p_0^*(x) = C_1 y_1(x) \quad (\text{SM52})$$

as the zero-order solution. For the first order, we obtain the inhomogeneous equation

$$\frac{d^2}{dx^2} p_1^*(x; z) + \frac{d}{dx} \left[p_1^*(x; z) \frac{U'(x)}{K_B \mathcal{T}} \right] = -\lambda_*(z) p_0^*(x). \quad (\text{SM53})$$

By the method of variation of parameters, the general solution of Eq. (SM53) is given by

$$p_1^*(x; z) = C_1 \lambda_*(z) \left[y_1(x) \int_{\xi_1}^x d\xi y_2(\xi) - y_2(x) \int_{\xi_2}^x d\xi y_1(\xi) \right], \quad (\text{SM54})$$

where ξ_1 and ξ_2 are arbitrary constants. As mentioned, the decay at $x \rightarrow -\infty$ should be exponential, hence the coefficient of $y_2(x)$ must vanish in this limit. Thus, we must choose $\xi_2 = -\infty$, which gives

$$p_*(x; z) \simeq C_1 y_1(x) + C_1 \lambda_*(z) \left[y_1(x) \int_{\xi_1}^x d\xi y_2(\xi) - y_2(x) \int_{-\infty}^x d\xi y_1(\xi) \right]. \quad (\text{SM55})$$

Setting this to zero at $x = z$ yields

$$\lambda_*(z) \simeq \frac{1}{Z} \left\{ \int_0^z dx \exp \left[\frac{U(x)}{K_B \mathcal{T}} \right] \right\}^{-1}, \quad (\text{SM56})$$

while further approximating this for $z \rightarrow \infty$, we find

$$\lambda_*(z) \sim \frac{1}{Z} \frac{U'(z)}{K_B \mathcal{T}} \exp \left[-\frac{U(z)}{K_B \mathcal{T}} \right]. \quad (\text{SM57})$$

Things are more complicated when the potential grows slower than linearly, i.e. $0 < \alpha < 1$ in Eq. (SM48), so that the force decays to zero for large x . Here, the spectrum of the Fokker-Planck equation on the semi-infinite domain $-\infty < x \leq z$ is not discrete, and the eigenvalues go continuously to 0. Treating this case requires a very different approach, which is beyond the scope of this paper. However, if we use a reflective boundary condition at $x = 0$, solving the problem of $x \in [0, z]$ instead, the spectrum is indeed discrete and we can proceed as before. Therefore, we now solve Eq. (SM46) over the domain $x \in [0, z]$, where the boundary conditions are $dp_*(x; z)/dx|_{x=0} = p_*(z; z) = 0$. The zero-order has the same general solution, and its boundary conditions read $p_0^{*'}(0) = p_0^*(\infty) = 0$. Since $y_2'(0) = 1$, we have the same solution for the zero-order. Hence, we obtain the same inhomogeneous equation for the first-order, solved via the method of variation of parameters to yield Eq. (SM54). However, this time due to the boundary condition at 0 and given that $y_2'(0) = 1$, we must choose $\xi_2 = 0$, and we obtain an eigenvalue which is twice the magnitude of the $\alpha > 1$ case, i.e. $2\lambda_*(z)$.

Note that for large z , the effective IID underlying CDF,

$$1 - F^{\text{iid}}(z) = \int_z^\infty dx P_{\text{eq}}(x) \propto \frac{1}{U'(z)} \exp \left[-\frac{U(z)}{K_B \mathcal{T}} \right], \quad (\text{SM58})$$

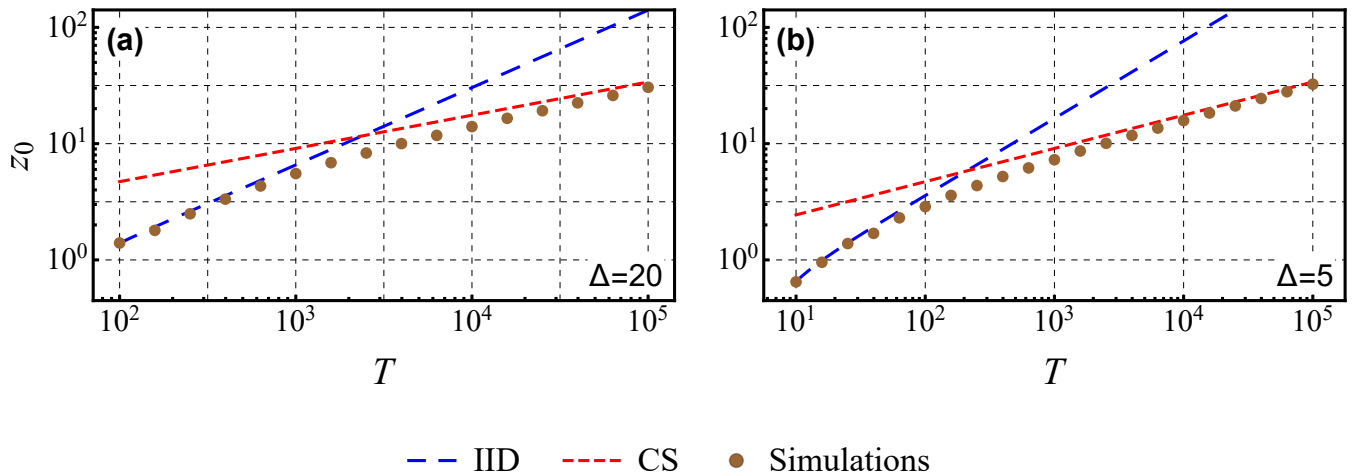


FIG. SM5. (Color online) **The Fréchet class:** The mode z_0 of a correlated stochastic process $x(t)$, evolving in time via the Langevin equation, Eq. (SM40), with a potential given by Eq. (SM70) with $\beta = 2.5$, for (a) $\Delta = 20$ and (b) $\Delta = 5$, where we set $D = a = 1$. Seen are stochastic simulations of the Langevin equation (brown disks), the IID limit given by solving Eq. (SM63) (dashed blue line), and the CS limit given by Eq. (SM69) (short-dashed red line). The CS limit dominates the DS EV distribution for large measurement times due to the force diminishing at $x \rightarrow \infty$, while for smaller T s the IID limit prevails. Each mode was calculated by maximizing a 10th-order polynomial fitted to a PDF constructed out of 10^5 EVs whose initial conditions are $x = 0$, obtained using the Euler–Maruyama method with an underlying time increment of 0.01 and a reflective boundary condition at $x = 0$.

differs from the CS effective CDF,

$$1 - F^{\text{cs}}(z) \propto \lambda_*(z) \propto U'(z) \exp\left[-\frac{U(z)}{K_B \mathcal{T}}\right], \quad (\text{SM59})$$

by a prefactor $\propto [U'(z)]^2$, proportional to $z^{2\alpha-2}$ as $z \rightarrow \infty$. Thus, for $0 < \alpha < 1$, the latter PDF decays faster than the former, which means that the average EV in the IID picture is larger than the CS one for large T . As $z_{\text{ds}} \leq z_{\text{cs}}$ dictates that $\langle z_{\text{ds}} \rangle \leq \langle z_{\text{cs}} \rangle$, one must infer that for forces which vanish at large distance, the asymptotic behavior at large- z is bounded from above by the CS limit, and hence it cannot approach the IID limit, in contradistinction to what happens for diverging forces, e.g. the OU model. For the case of $\alpha = 1$, namely an asymptotically linear potential, the $z^{2\alpha-2}$ prefactor is absent. In this case, both the effective IID EV distribution and its CS limit counterpart are asymptotically purely exponential. This linear potential case was discovered to be marginal also for other problems which are not related to DS, see for example Ref. [SM6], where the authors find a freezing transition in the long-time decay rate of the first-passage distribution of a particle whose trajectory is controlled by Eq. (SM40). Lastly, we stress that due to the exponential-like decay of the IID underlying CDF and of the CS effective CDF, both limits belong to the Gumbel class for any $\alpha > 0$, hence the associated DS processes are probably of an identical nature.

The above results are demonstrated in Fig. 4, where we assumed the following shape for the potential,

$$U(x) = \frac{1}{\alpha}(1+x^2)^{\alpha/2} \quad (\text{SM60})$$

with $D = K_B \mathcal{T} = 1$, which has the same asymptotics as Eq. (SM48). The IID curves were computed from Eq. (SM42), while the CS curves from Eq. (SM47), with $\lambda_*(z)$ given by Eq. (SM56). For the OU model of $\alpha = 2$ we used the exact solution for $\lambda_*(z)$, given using the parabolic cylinder function just above Eq. (5) in the main text. When $\alpha < 1$, we accounted for the reflection at $x = 0$ by replacing $Z \rightarrow Z/2$ in the IID and CS formulas, Eqs. (SM42) and (SM56), respectively.

The Fréchet class

The Fréchet class occurs when $P_{\text{eq}}(x) \propto x^{-\beta}$ for $x \rightarrow \infty$ and $\beta > 1$. We assume the following large- $|x|$ behavior for the potential,

$$U(x) \sim U_\infty \ln(|x|/a), \quad U_\infty > 0, \quad a > 0, \quad (\text{SM61})$$

where $\beta \equiv U_\infty/(K_B\mathcal{T}) > 1$, such that for large enough z we have for the EV IID limit,

$$F_N^{\text{iid}}(z) \simeq \left[1 - \frac{1}{Z} \int_z^\infty dx \left(\frac{a}{x} \right)^\beta \right]^N = \left[1 - \frac{a^\beta z^{1-\beta}}{(\beta-1)Z} \right]^N. \quad (\text{SM62})$$

Note that depending on β , the mean is not always well-defined. Hence, here we use the mode z_0 of the EV PDF as an observable. For single maximum PDFs, it is defined as

$$\left. \frac{d}{dz} \text{PDF}(z) \right|_{z=z_0} = 0. \quad (\text{SM63})$$

Thus, when N is large we obtain the EV mode in the IID limit,

$$z_0^{\text{iid}}(N) \simeq a \left[\frac{a N(\beta-1) + 1}{Z \beta(\beta-1)} \right]^{1/(\beta-1)}. \quad (\text{SM64})$$

We now move to the CS limit. In Ref. [73], the authors presented an approximation to $p_\lambda(x; z)$ with $z \rightarrow \infty$ for a potential behaving as Eq. (SM61). By moving to the Schrödinger representation,

$$\psi_k(x; z) \equiv \frac{p_\lambda(x; z)}{\sqrt{P_{\text{eq}}(x)}}, \quad k \equiv \sqrt{\lambda}, \quad (\text{SM65})$$

they found that in the large- x regime, up to a normalization constant

$$\psi_k(x; z \rightarrow \infty) \simeq \sqrt{\frac{x}{a}} \left[-\Gamma(\nu) \frac{Z}{a} \left(\frac{ka}{2} \right)^{2-\nu} J_\nu(kx) + \Gamma(1-\nu) \left(\frac{ka}{2} \right)^\nu J_{-\nu}(kx) \right], \quad \nu \equiv \frac{\beta+1}{2}, \quad (\text{SM66})$$

where $J_\nu(\cdot)$ is Bessel's function of the first kind, see Eqs. (38), (40), and (50) of Ref. [SM7]. To obtain the solution for a finite z , here we need to change the upper boundary condition from $x = \infty$ to $x = z$. This can be done simply by demanding that $\psi_k(z; z \rightarrow \infty) = 0$ for a certain $k_*(z)$. Using the small argument expansion of the Bessel function, $J_\nu(\xi) \sim (\xi/2)^\nu / \Gamma(\nu+1)$, we obtain

$$\lambda_*(z) = k_*^2(z) \simeq \frac{4\nu}{a^2} \frac{a}{Z} \left(\frac{a}{z} \right)^{2\nu}. \quad (\text{SM67})$$

Plugging this into Eq. (SM47) yields the CS EV CDF, which for large z behaves as

$$F_T^{\text{cs}}(z) \simeq \left[1 - 2(\beta+1) \frac{a}{Z} \left(\frac{a}{z} \right)^{\beta+1} \right]^{DT/a^2}, \quad (\text{SM68})$$

from which the mode is found for large T ,

$$z_0^{\text{cs}}(T) \simeq a \left[\frac{(1+\beta)^2 DT}{1+\beta/2} \frac{DT}{aZ} \right]^{1/(\beta+1)}. \quad (\text{SM69})$$

Note that the derivation presented in Ref. [SM7] assumes an even wave function for the perturbative solution of the small- x inner region. Consequently, the above expressions are valid when a reflective boundary condition at the origin is assumed, i.e. $0 \leq x \leq z$, as with the $0 < \alpha < 1$ case of the Gumbel domain. A semi-infinite case of $x \in (-\infty, z]$ can be treated by generalizing the results obtained in Ref. [SM7] for the solution of $\psi_k(x; z \rightarrow \infty)$ in the small- x regime for a general parity wave function, which is again beyond the scope of this paper. Also, we see that the IID underlying CDF, $1 - F^{\text{iid}}(z) \propto z^{-\beta+1}$, differs from the CS effective CDF, $1 - F^{\text{cs}}(z) \propto z^{-\beta-1}$, by a prefactor $\propto z^{-2}$. Thus, for any $\beta > 1$, the latter PDF decays faster than the former, and by the same argument made for processes that belong to the Gumbel class with $0 < \alpha < 1$, one infers that DS processes which belong to the Fréchet class cannot converge to their respective IID limits when T becomes large, in contradistinction to processes which belong to the Gumbel class with $\alpha > 1$, or to processes attracted to the Weibull class (for the latter, see below). One can also see that both the IID and CS limits above lie in the Fréchet domain, as the respective CDFs decay as a power-law.

We put these predictions to a test using the potential

$$U(x) = \frac{\beta}{2} \ln(1+x^2), \quad (\text{SM70})$$

which for large x behaves as Eq. (SM61) with $a = 1$. Setting $\beta = 2.5$ and $D = 1$, we find that for large T s the CS limit dominates the EV distribution, whereas for smaller T s the IID picture wins, as depicted in Fig. SM5. We accounted for the reflection at $x = 0$ by setting $Z \rightarrow Z/2$ in the IID expression.

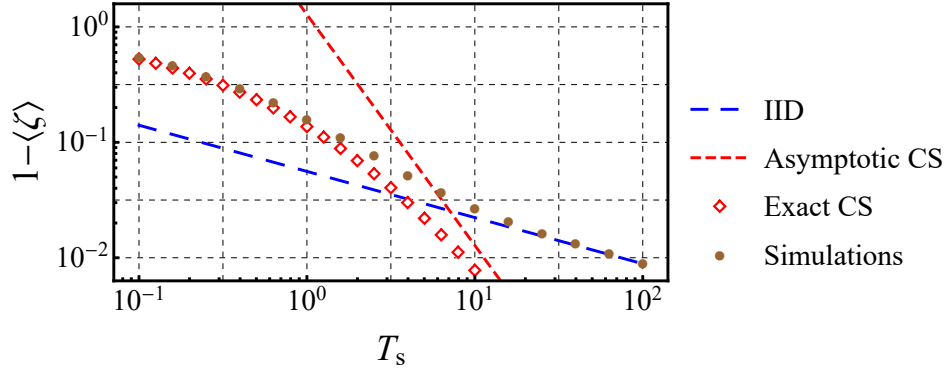


FIG. SM6. (Color online) **The Weibull class:** The observable $1 - \langle \zeta \rangle$ of a correlated stochastic process $x(t)$, evolving in time via the Langevin equation, Eq. (SM40), with a potential given by Eq. (SM71), where $\gamma = 2.5$ and $\Delta_s \equiv D\Delta/L^2 = 10^{-3}$. Seen are stochastic simulations of the Langevin equation (brown disks), the IID limit given by Eq. (SM75) (dashed blue line), the long-time asymptotics of the CS limit given by Eq. (SM84) (short-dashed red curve), and the exact CS limit obtained by numerically solving the time-dependent Fokker-Planck equation, Eq. (SM43) (hollow red squares). A clear transition from the CS limit to the IID prediction can be observed when the overall scaled measurement time $T_s \equiv DT/L^2$ is increased. Each mean is made of 10^4 maxima, whose initial conditions are $x = 0$, obtained using the Euler–Maruyama method with a varying underlying time increment with a maximal magnitude of 10^{-5} , and a reflective boundary condition at $x = 0$.

The Weibull class

The Weibull class occurs when there is a finite upper bound L on the interval in which the particle is allowed to travel and $P_{\text{eq}}(x)$ decays slowly enough for $x \rightarrow L$. As the particle’s movement is bounded, its maximum value cannot exceed L , hence it proves useful to study the value $L - \langle z \rangle$. Here, we consider the following example case,

$$U(x) = \begin{cases} U_0 \ln\left(\frac{L}{L-x}\right) & 0 \leq x \leq L \\ \infty & \text{otherwise} \end{cases}, \quad (\text{SM71})$$

such that $L > 0$ and $\gamma \equiv 1 + U_0/(K_B\mathcal{T}) > 0$. Note that $\gamma = 1$ corresponds to $U_0 = 0$, i.e. to a particle diffusing in a box, which is solved below. For now, let us write down the IID equilibrium measure,

$$P_{\text{eq}}(x) = \frac{\gamma}{L} \left(1 - \frac{x}{L}\right)^{\gamma-1}, \quad (\text{SM72})$$

which can be rescaled as $Q_{\text{eq}}(\chi)d\chi \equiv P_{\text{eq}}(x)dx$ with $x = L\chi$, such that L vanishes from the expressions,

$$Q_{\text{eq}}(\chi) = \gamma(1-\chi)^{\gamma-1}, \quad F^{\text{iid}}(\chi) = 1 - (1-\chi)^\gamma. \quad (\text{SM73})$$

The IID limit of the DS EV CDF is thus,

$$F_N^{\text{iid}}(\zeta) = [1 - (1-\zeta)^\gamma]^N, \quad (\text{SM74})$$

where $\zeta \equiv z/L$, which yields

$$1 - \langle \zeta \rangle_{\text{iid}} = 1 - \int_0^1 d\zeta \left[\frac{d}{d\zeta} F_N^{\text{iid}}(\zeta) \right] \zeta = \frac{\Gamma(1+1/\gamma)\Gamma(1+N)}{\Gamma(1+1/\gamma+N)} \sim \Gamma\left(1 + \frac{1}{\gamma}\right) N^{-1/\gamma} = \Gamma\left(1 + \frac{1}{\gamma}\right) \left(\frac{\Delta}{T}\right)^{1/\gamma}, \quad (\text{SM75})$$

namely a power-law decay for large T with an exponent of $1/\gamma$.

Similarly to the Gumbel case with $\alpha > 1$, the CS prediction is entirely off for large measurement times, starting from a power-law decay of a different exponent for $\gamma > 2$, and ending with an exponential-like decay when $0 < \gamma < 2$. To compute this behavior, we rewrite the rescaled Fokker-Planck eigenvalue equation, based of Eq. (SM46),

$$\frac{d^2}{d\chi^2} q_\kappa(\chi; \zeta) + \frac{d}{d\chi} \left[q_\kappa(\chi; \zeta) \frac{\gamma-1}{1-\chi} \right] + \kappa^2(z) q_\kappa(\chi; \zeta) = 0, \quad (\text{SM76})$$

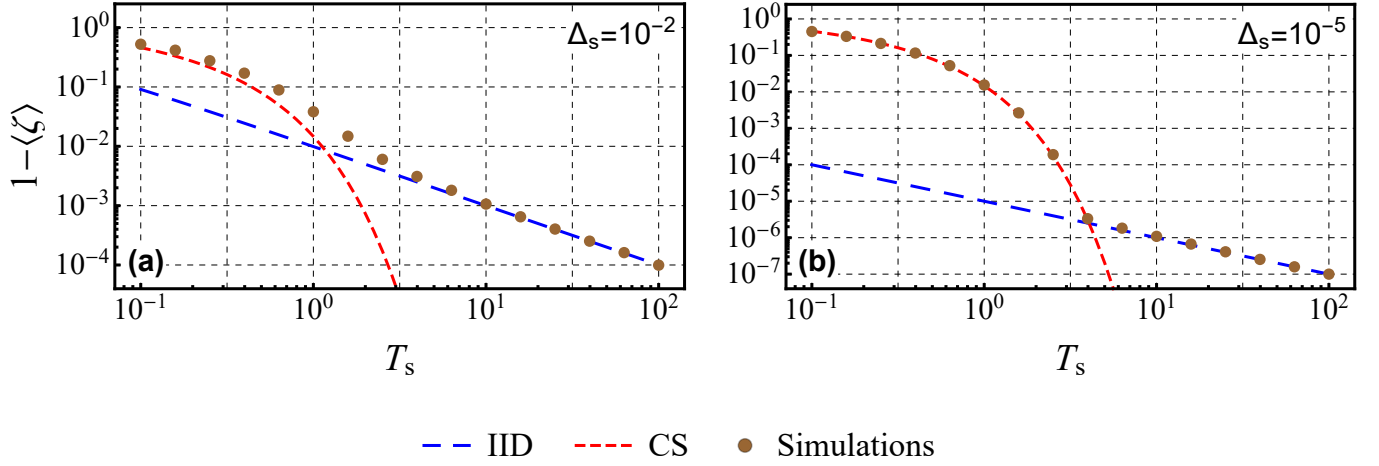


FIG. SM7. (Color online) **Particle diffusing in a box:** The observable $1 - \langle \zeta \rangle$ of a particle confined to $[0, 1]$ and controlled by the Langevin equation, Eq. (SM40), with a potential given by Eq. (SM71) where $\gamma = 1$, for (a) $\Delta_s \equiv D\Delta/L^2 = 10^{-2}$ and (b) $\Delta_s = 10^{-5}$. Seen are stochastic simulations of the Langevin equation (brown disks), the IID limit given by Eq. (SM75) (dashed blue line), and the CS limit given by Eqs. (SM86) and (SM88) (short-dashed red curve). A clear transition from the CS limit to the IID limit can be observed when the overall scaled measurement time $T_s \equiv DT/L^2$ is increased. When decreasing Δ_s , the transition occurs at a larger T_s . Each mean is made of 10^4 maxima whose initial conditions are $x = 0$, obtained using the Euler-Maruyama method with an underlying time increment of 10^{-6} and reflective boundary conditions at $x = 0$ and $x = 1$.

with $\kappa = L\sqrt{\lambda}$ and $q_\kappa(\chi; \zeta)d\chi = p_k(x; z)dx$. This equation can be solved using the Bessel functions similarly to the Fréchet example above, yielding the general solution

$$q_\kappa(\chi; \zeta) = [\kappa(1 - \chi)]^{\gamma/2} \{AJ_\epsilon[\kappa(1 - \chi)] + BJ_{-\epsilon}[\kappa(1 - \chi)]\}, \quad \epsilon \equiv \frac{\gamma - 2}{2}. \quad (\text{SM77})$$

The boundary conditions which we impose are reflection at $\chi = 0$, which determines B in terms of A , and absorption at $\chi = \zeta$, which yields $\kappa(\zeta)$, namely

$$\left. \frac{d}{d\chi} q_\kappa(\chi; \zeta) \right|_{\chi=0} + (\gamma - 1)q_\kappa(0; \zeta) = 0, \quad q_\kappa(\zeta; \zeta) = 0. \quad (\text{SM78})$$

These conditions give

$$B = \frac{AJ_{\epsilon+1}(\kappa)}{J_{-\epsilon-1}(\kappa)}, \quad (\text{SM79})$$

and

$$J_{-\epsilon-1}(\kappa)J_\epsilon[\kappa(1 - \zeta)] + J_{\epsilon+1}(\kappa)J_{-\epsilon}[\kappa(1 - \zeta)] = 0, \quad (\text{SM80})$$

where the latter can be expanded for $\zeta \rightarrow 1$,

$$\Gamma(\epsilon + 1)J_{\epsilon+1}(\kappa) + \left[\frac{\kappa(1 - \zeta)}{2} \right]^{\gamma-2} \Gamma(1 - \epsilon)J_{-\epsilon-1}(\kappa) = 0. \quad (\text{SM81})$$

Therefore, we see that one needs to separately consider two cases, as mentioned. For $\gamma > 2$, the smallest root of Eq. (SM81) is obtained for small κ , and thus by expanding we find

$$\kappa_*^2(\zeta) \simeq \gamma(\gamma - 2)(1 - \zeta)^{\gamma-2}, \quad (\text{SM82})$$

which decay to 0 when $\zeta \rightarrow 1$. This gives for the CS limit of the DS EV CDF

$$F_T^{\text{CS}}(\zeta) \sim \exp \left[-\gamma(\gamma - 2)(1 - \zeta)^{\gamma-2} T_s \right] \simeq \left[1 - \gamma(\gamma - 2)(1 - \zeta)^{\gamma-2} \right]^{T_s}, \quad (\text{SM83})$$

where $T_s \equiv DT/L^2$, and the subscript ‘‘s’’ stands for ‘‘scaled’’. This yields

$$1 - \langle \zeta \rangle_{cs} \simeq \Gamma \left(\frac{\gamma - 1}{\gamma - 2} \right) \left[\gamma(\gamma - 2)T_s \right]^{-1/(\gamma-2)}, \quad (\text{SM84})$$

namely a different power-law decay with an exponent of $1/(\gamma - 2)$. On the other hand, taking $0 < \gamma < 2$, we see that the second term of Eq. (SM81) diverges when $\zeta \rightarrow 1$. Hence, the smallest root is found roughly as the first solution of $J_{-\epsilon-1}(\kappa) = 0$. This is a positive number independent of ζ , which means that the decay of $1 - \langle \zeta \rangle_{cs}$ is exponential-like for $0 < \gamma < 2$.

To illustrate these results, we first set $\gamma = 2.5$ in Fig. SM6. Plotting $1 - \langle \zeta \rangle$ versus the overall scaled measurement time T_s , we see that even if one takes a small sampling time of $\Delta_s \equiv D\Delta/L^2 = 10^{-3}$, the CS limit fails for large T_s , and the IID RVs limit takes control of the EVs, with an underlying distribution which is the equilibrium measure. For the other regime, we set $\gamma = 1$, giving the example of a particle diffusing in a box, as mentioned. Using Eq. (SM75), the IID prediction for our observable display a power-law decay of $1/T_s$ for large T_s . Alternatively, the CS limit is obtained by solving the time-dependent Fokker-Planck equation, Eq. (SM43), with a left boundary condition of $dq(\chi, t_s|\zeta)/d\chi|_{\chi=0} = 0$, where $t_s \equiv Dt/L^2$ is the rescaled time. This gives

$$q(\chi, t_s|\zeta) = \sum_{m=0}^{\infty} \frac{2}{\zeta} \cos \left[(1 + 2m) \frac{\pi\chi}{2\zeta} \right] \exp \left[-(1 + 2m)^2 \frac{\pi^2 t_s}{4\zeta^2} \right], \quad (\text{SM85})$$

and so

$$F_{T_s}^{cs}(\zeta) = \int_0^{\zeta} d\chi q(\chi, T_s|\zeta) = \sum_{m=0}^{\infty} \frac{4/\pi}{1 + 2m} \exp \left[-(1 + 2m)^2 \frac{\pi^2 T_s}{4\zeta^2} \right]. \quad (\text{SM86})$$

Surprisingly, this representation for the EV CDF in the CS limit is incomplete, since in the truly continuous case, the (rescaled) upper bound on the particle’s movement means that from a certain time and onward, the EV of any realization of the process becomes equal to 1. This suggests that there is a $\delta(\zeta - 1)$ contribution to the EV PDF with a time-dependent weight. This is further evidenced by noting that $F_{T_s}^{cs}(1) < 1$ for T_s large enough, i.e. this distribution is not normalized. Incorporating this observation into the calculation is relatively straightforward. We simply write

$$\frac{d}{d\zeta} F_{T_s}^{cs, \text{true}}(\zeta) = \frac{d}{d\zeta} F_{T_s}^{cs}(\zeta) + [1 - F_{T_s}^{cs}(1)] \delta(\zeta - 1), \quad (\text{SM87})$$

which is indeed normalized to unity. Our observable in the CS limit is then

$$1 - \langle \zeta \rangle_{cs} = 1 - \int_0^1 d\zeta \left[\frac{d}{d\zeta} F_{T_s}^{cs, \text{true}}(\zeta) \right] \zeta = \int_0^1 d\zeta F_{T_s}^{cs}(\zeta). \quad (\text{SM88})$$

In the $T_s \rightarrow \infty$ limit, we find

$$1 - \langle \zeta \rangle_{cs} \sim \frac{8}{\pi^3 T_s} \exp \left(-\frac{\pi^2}{4} T_s \right), \quad (\text{SM89})$$

namely an exponential decay for large T_s . Note that the first solution of $J_{-1/2}(\kappa_*) = 0$ is exactly the effective $\kappa_* = \pi/2$ above. Figure SM7 shows $1 - \langle \zeta \rangle$ versus the scaled overall measurement time T_s for a particle diffusing in a box. It is clear that the CS limit fails for large T_s , while the IID limit works excellently. This marks a qualitative difference between a DS with any finite Δ_s to the CS limit of $\Delta_s = 0$, also for this example of particles in a box. Moreover, the required addition of the delta function suggests that the Weibull universality class is no longer an attractor for the continuous process, even though the IID limit does belong there. This change in the basin of attraction has interesting consequences, and is a worthy subject for a future research.

[SM1] S. N. Majumdar, A. Pal, and G. Schehr, *Phys. Rep.* **840**, 1 (2020).

[SM2] See the identity at functions.wolfram.com/05.01.23.0013.01 with $z = x/\sqrt{2}$, $z_1 = x'/\sqrt{2}$, and $w = \mu/2$.

[SM3] One can prove Eq. (SM27) by differentiating it with respect to μ , and using $\text{He}_n(x) = x\text{He}_{n-1}(x) - \text{He}'_{n-1}(x)$ together with Eq. (SM25) to show that the resulted expression holds. Verifying that Eq. (SM27) is satisfied for $\mu = 0$ concludes the proof.

- [SM4] Equation (SM36) can be proved by differentiating it with respect to z , and verifying that the resulted expression is satisfied by using $\text{He}_n(x) = x\text{He}_{n-1}(x) - \text{He}'_{n-1}(x)$ and the identity found at <http://functions.wolfram.com/05.01.16.0006.01>. Showing that Eq. (SM36) holds for $z \rightarrow -\infty$ concludes the proof.
- [SM5] B. V. Bondarev, *App. Math.* **8**, 1529 (2017).
- [SM6] S. Sabhapandit and S. N. Majumdar, *Phys. Rev. Lett.* **125**, 200601 (2020).
- [SM7] A. Dechant, E. Lutz, E. Barkai, and D. A. Kessler, *J. Stat. Phys.* **145**, 1524 (2011).